Simultaneous Interpenetrating Networks of a Polyurethane and Poly(methyl methacrylate). I. Metastable Phase Diagrams

V. MISHRA,[1,3,4] F. E. DU PREZ,[6] E. GOSEN,[2] E. J. GOETHALS,[6] and L. H. SPERLING[1-5,*]

[1]Department of Chemical Engineering, [2]Department of Materials Science and Engineering, [3]Center for Polymer Science and Engineering, [4]Materials Research Center, [5]Polymer Interfaces Center, Lehigh University, Bethlehem, Pennsylvania 18015; and [6]Department of Organic Chemistry, Polymer Chemistry Division, University of Ghent, Krijgslaan 281 S4-bis B-9000, Ghent, Belgium

SYNOPSIS

Any simultaneous interpenetrating network (SIN) synthesis contains three key events. These are gelation of polymer I, gelation of polymer II, and phase separation of polymer I from polymer II. Metastable phase diagrams of SINs are developed, in which the time occurrence of these three events is represented. A polyurethane/poly(methyl methacrylate) (PU/PMMA) system was chosen as a model. Polymerization kinetics were followed *in situ* for both PU and PMMA using Fourier Transform Infrared Spectroscopy (FTIR) with the aid of a heated demountable cell. Glass transitions of fully cured samples were determined by dynamic mechanical spectroscopy (DMS) and differential scanning calorimetry (DSC). Phase separation was determined by the onset of turbidity, and gelation of the first gelling polymer was determined by the sudden resistance of the system to flow. As a result, a metastable phase diagram was constructed for the four-component SIN system (the two monomers and their respective polymers) as a tetrahedron in three dimensions with the two monomers and two polymers at the four apexes. Phase separation and gelations of the two polymers are indicated by various surfaces. These surfaces intersect at lines and curves, representing unique conditions of an SIN synthesis, e.g., simultaneous gelation of both polymers, or simultaneous phase separation and gelation of polymer I, etc. These conditions are critical in terms of the development of the SIN morphology, dividing the reaction space into specific regions. Finally, it is shown how the tetrahedron diagram helps visualize the course of the three key events during SIN synthesis, and provides direction for controlling them.

INTRODUCTION

Interpenetrating polymer networks (IPNs) are defined as a combination of two or more polymers in network form, at least one of which is synthesized and/or crosslinked in the immediate presence of the other.[1,2] Based on synthetic routes, IPNs have traditionally been classified into two subclasses. The first, sequential IPNs, are made by swelling polymer network I with a monomer mixture II, followed by polymerization of the latter. The second, simultaneous interpenetrating networks (SINs), are obtained when all monomers or prepolymers and their corresponding crosslinkers are first mixed together, before polymerization of either component. Such systems require noninterfering routes for the two polymerizations. A major thermodynamic difference between the sequential IPNs and SINs is that network I in the former is stretched due to the swelling step, whereas in the latter, both networks are more or less relaxed. The polymer that gels first in SINs, and network I in sequential IPNs, tends to form the more continuous phase.

* To whom correspondence should be addressed at Lehigh University, Materials Research Center, Whitaker Laboratory, 5 E. Packer Avenue, Bethlehem, PA 18015-3194.

Journal of Applied Polymer Science, Vol. 58, 331-346 (1995)
 CCC 0021-8995/95/020331-16

PU–PMMA SINs

There are over 50 articles regarding SINs of a polyurethane (PU), and an acrylic or styrenic polymer.[2] Among these articles, the most visible are the PU/poly(methyl methacrylate) (PMMA) SINs, because this system gives good mechanical and damping properties, while also serving as an excellent model SIN system. For example, Kim et al.[3,4] studied PU/PMMA SINs and found that phase domains were finer in SINs than in the corresponding linear blends and that the two glass transitions (T_gs) were shifted inward. Meyer and co-workers[5,6] found even larger inward shifts in the T_gs of their SINs of the same system (e.g., 43°C vs. 15°C, for about 50/50 compositions). Significant broadening of the transitions was also noted along with improvements in some mechanical properties. Later, Hur et al.[7,8] obtained extremely broad, single glass transitions in their investigation. Very recently, Akay and Rollins[9,10] found that varying the overall SIN composition could give from two shifted T_gs to a single broad T_g. Lastly, SINs from the current work show two distinct T_gs with no measurable inward shifting.

Due to differences in glass transition behavior, different authors concluded different levels of interactions and mixing between the two phases. The corresponding mechanical property studies[6–8,10] as well as morphology (TEM) studies[3,11] accentuated these differences. Of course, the polyurethanes used in these studies were not always identical, making the comparisons difficult. But an inspection of all the systems clearly indicates that the differences noted arise because of the different polymerization conditions employed. Indeed, Tabka et al.[12,13] recently found that noticeable differences in the morphology and the damping behavior of PU/PMMA SINs can be obtained by changing the relative reaction kinetics of the two polymers. Depending on the concentration of the catalyst for the PU, for the same overall SIN composition, different morphologies were obtained, ranging from a very fine phase dispersion to more or less individualized domains. Dynamic mechanical spectroscopy (DMS) confirmed these results, showing either a single broad transition or two well-defined peaks in tan δ ($= G''/G'$, where G'' and G' represent the loss and storage shear moduli, respectively). The present study was undertaken to understand further the conditions that cause the same system to result in different morphologies and properties.

Metastability in phase morphology of IPNs was noted by Zhou and co-workers[14–16] for the poly(carbonate-urethane)/polystyrene (PCU/PS) system. Using differential scanning calorimetry (DSC), it was found that some of the IPN samples changed slowly from a single phase to a two-phase morphology over a period of 8 months.[14,16] The initially miscible state was termed a metastable state, which reflects the high degree of entanglement of the linear polystyrene chains with the PCU network.[14–16] The net effect was a limited molecular mobility and greatly retarded phase separation in the otherwise immiscible PCU/PS system. By contrast, the PCU/PMMA SINs were found to be stable, one-phased materials for up to 2.5 years.[14]

In SIN syntheses generally, there are three key events, gelation of polymer I, gelation of polymer II, and phase separation of polymer I from II. The relative positions of these three events along reaction time ought to be extremely important in the development of morphology, and hence, properties of the product. However, in spite of the numerous studies on SINs and sequential IPNs in general, the amount of literature addressing their gelation and phase separation remains extremely small. In part, this is due to the presence of crosslinks, which rarely allow thermodynamic equilibrium with respect to phase separation. Therefore, in a strict sense, phase diagrams cannot be constructed. But this leaves much to be desired in terms of understanding the phase behavior of SIN and IPN systems. In this article, it is proposed that *metastable* phase diagrams be defined and developed for IPNs/SINs, which will describe the conditions under which gelation of one polymer may be caused to precede or follow the other, and under which conditions phase separation precedes or follows one or both gelations.

EXPERIMENTAL

Synthesis

All samples were synthesized in an oven at 60°C in molds prepared with cleaned glass plates, sprayed with a TFE-based mold release agent and then baked at 250°C for an hour. Upon cooling, two such plates were clamped together with a 3 mm thick Teflon™ spacer. All materials and proportions used are summarized in Table I.

Polyurethane Network

PPG diol and TMP triol were charged in 1 : 1 equivalent ratio to a glass jar equipped with a mechanical stirrer in a 60°C bath. The charge was stirred under vacuum for 30 min to remove dissolved water from PPG and TMP. This was also sufficient time to dis-

Table I SIN Materials and Recipes Used

Compound	Class	Amount	Supplier
PU			
Poly(oxypropylene)glycol (PPG); MW = 2000.	polyether diol	1.0 equiv.	Polysciences
Dicyclohexylmethane-4,4'-diisocyanate (H_{12}MDI), Desmodur W.	aliphatic diiocyanate	2.0 equiv.	Miles, Inc.
2-Ethyl-2-(hydroxymethyl)-1,3-propane diol, or, Trimethylolpropane (TMP).	crosslinker	1.0 equiv.	Aldrich
2-Butyl-2-ethyl-1,3-propanediol (BEPD).	chain extender	1.0 equiv.	Eastman Chemical
Dibutyl tin dilaurate (T-12).	tin catalyst	0.05% (w/wPU)	Aldrich
PMMA			
Methyl methacrylate (MMA)	monomer	96.5–99.0%	Aldrich
Tetraethylene glycol dimethacrylate (TEGMD)	crosslinking monomer	0.5–3.0%	Polysciences
Lauroyl peroxide (LPO)	initiator	0.5%	Aldrich
PS			
Styrene (Sty)	monomer	96.5%	Aldrich
Divinyl benzene (DVB), 55% purity	crosslinking monomer	3.0%	Aldrich
Lauroyl peroxide (LPO)	initiator	0.5%	Aldrich

Polymerization Temperature = 60°C.

solve TMP completely in PPG. The jar was removed, tightly closed, and allowed to cool to room temperature. Then it was charged with two equivalents of H_{12}MDI and 0.05% (wt/wt of PU) T-12 catalyst (added as a 5% solution in toluene), followed by vigorous stirring for 5–10 min in vacuum to avoid any air intake. The resulting PU reaction mix, further referred to as "U," was then charged to a mold and polymerized in an oven at 60°C. For the corresponding linear PU, the TMP triol was replaced with an equivalent amount of BEPD diol.

PMMA Network

The MMA and TEGDM monomers were passed through neutral aluminum oxide columns (alumina, Brockmann Activity I, Aldrich Chemical Co.) to remove inhibitors and stored below 0°C until use. The monomers and LPO initiator were mixed in the desired proportions at room temperature, followed by flushing with dry N_2 gas to remove dissolved oxygen (O_2) gas. The mixture was quickly degassed in vacuum and poured into the mold, followed by polymerization at 60°C for about 10 h. Postcuring was done at 100°C for 4 h followed by 120°C in vacuum for another 10 h.

For preparing linear PMMA, no crosslinking monomer TEGDM was added. A linear PMMA (IRD-2) of M_n = 42,000 g/mol was also obtained from Rohm & Haas Co. for phase diagram model studies. The molecular weights (MWs) of both types of PMMA were determined using a Waters Gel Permeation Chromatograph (GPC) with a polystyrene (PS) calibration in tetrahydrofuran medium. The equivalent PS MWs are reported.

Polystyrene Network

For comparison, some SINs based on polystyrene (PS) instead of PMMA were also prepared. Styrene and DVB monomers were treated by neutral alumina and stored in the same manner as the methacrylates. However, unlike the methacrylates, the inhibitor removal was only partial for the styrenic monomers, as indicated by the subsequent FTIR-polymerization experiments. The polymerization methods were identical to those for the PMMA networks.

Simultaneous Interpenetrating Networks (SINs)

The PU–monomer mix, "U," and the acrylic or styrenic monomer mix were separately prepared as

described above and then mixed in the desired proportions. Mixing was done at room temperature in a glass jar by vigorous agitation. During mixing, a vacuum was applied to the reaction mixture for a few seconds and then released by flushing with dry N_2 gas. This step was repeated two to three times to effectively remove the dissolved O_2. A final application of vacuum for about 30–60 s was required for degassing, after which the mold was filled and placed in the oven at 60°C. The postcuring sequence was identical to that for the PMMA network.

Polymerization Kinetics by FTIR

Polymerization kinetics studies were performed *in situ* on a Mattson–Polaris Fourier Transform Infrared Spectrometer (FTIR) using a special heated demountable cell (HT-32; Spectra-Tech, Inc.). The cell contained two NaCl discs (32 mm diameter) with a Teflon™ spacer (0.025 mm thick). Temperature control of ±0.5°C was achieved by the use of a microprocessor-based PID temperature controller (CN9111A; Omega Inc.), which was manually tuned for the FTIR cell.

The cell was assembled and placed in the FTIR chamber and then heated to the reaction temperature of 60°C. Normally, 1 h was allowed for the cell to attain uniform temperature. Then, a part (< 0.1 mL) of freshly prepared reaction mixture was injected into the cell, the time taken as zero, and then, spectra taken at fixed intervals of time (see Fig. 1). The sample here is the initial reaction mixture (reaction time = 0 min) for a 50/50 PU/PMMA SIN. The peak heights at 1639 cm^{-1} and 2264 cm^{-1} are proportional to the concentrations of the —C=C— bonds (in MMA and TEGDM) and —N=C=O groups (in the diisocyanate), respectively. With increasing reaction time, these peaks drop in height, following Beer's law, thus enabling the generation of conversion vs. time plots for PMMA and PU, respectively. For experiments with styrene and DVB, the —C=C— peak at 908 cm^{-1} was chosen because the peak around 1639 cm^{-1} is too close to the phenyl peak at 1601 cm^{-1}.

Phase Separation and Gelation

The time of phase separation was determined visually by noting the onset of turbidity. All samples were initially clear, and usually turned turbid over a period of time of less than a minute.

To determine gelation times, a small glass vial (of 8 mL capacity) was filled with about 5 mL of initial mixture, sealed, and placed in the oven at 60°C. It was inspected at noted intervals of time (1–2 min near gelation) to determine the point at which the liquid stopped flowing upon vial inversion (gelation point). Normally, gelation also occurred within a time frame of about 1–2 min.

One minute of polymerization time corresponds approximately to a maximum MMA conversion of 1.3%, as estimated from the highest polymerization rate of pure PMMA in FTIR experiments.

Phase Diagrams

Ternary phase diagrams for the system MMA–PMMA–"U" were developed using two methods classified by the type of PMMA used: premixed and *in situ* polymerized.

Preliminary Studies: Premixed PMMA

For preliminary studies, the premixed method was used, in which the lower MW linear PMMA (IRD-2) was dissolved in inhibited MMA monomer (in concentrations up to 30% polymer by wt). A PU–monomer mix, "U," without the T-12 catalyst was used. Then, the MMA/PMMA solution was titrated with "U" until the mixture became cloudy. Because the viscosities of the solutions were high, the mixture was heated to 100°C for every composition to facilitate initial mixing and then cooled to the test temperature to check for appearance of cloudiness.

In Situ Polymerized PMMA

For the actual SIN system, the MMA/PMMA solutions are not smooth liquids, but rather gels (above the gelation points). Therefore, they cannot be uniformly mixed with "U" in accurate proportions physically as in the premixed method described above. So, the mixture "U" was dissolved in various amounts of the unreacted (liquid) MMA–monomer mix, containing LPO initiator. Subsequent heating of these mixtures to 60°C initiated the *in situ* polymerizations of MMA, during which, the times of phase separation were determined as explained above. For each MMA/"U" composition, the initial liquid reaction mixture was also injected into the FTIR cell and the MMA conversion vs. time curve determined as explained above. Thus, the MMA conversion at phase separation was determined for various "U" contents, with which a metastable phase diagram could be constructed. The absence of the T-12 catalyst in the component "U" was important in these experiments to restrict its undesirable polymerization to PU.

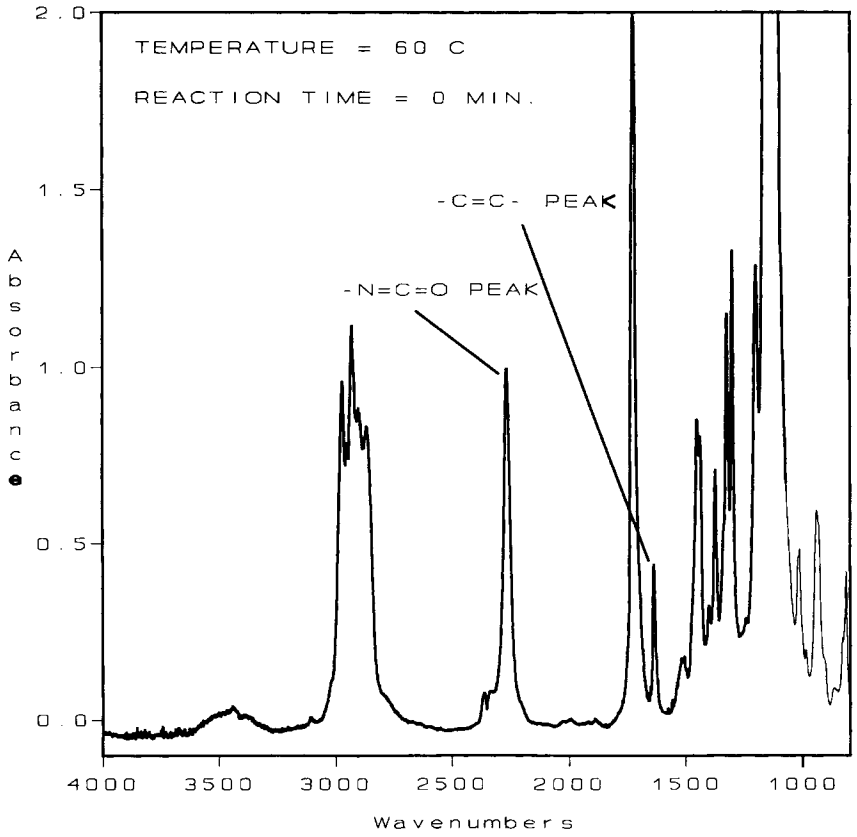

Figure 1 FTIR absorbance spectrum of the reaction mixture of a 50/50 SIN of PU/PMMA at the start of reactions. —N=C=O peak (diisocyanate) at 2264 cm^{-1} and —C=C— peak (MMA) at 1639 cm^{-1} are indicated.

A ternary phase diagram for the system MMA–PMMA–PU was also developed using the *in situ* polymerized method. However, the PU had to be linear instead of crosslinked because the PU–MMA mixture must be a liquid in order to be injected in the FTIR cell for the kinetics experiments. A linear PU (M_n = 90,000 g/mol) was prepared and dissolved in the PMMA–monomer mix and the same procedure described above for the system MMA–PMMA–"U" was followed.

Glass Transitions

Glass transitions (T_gs) of fully cured samples were determined by dynamic mechanical spectroscopy (DMS) on a Rheometrics Dynamic Analyzer II (RDA-II), and differential scanning calorimetry (DSC) on a Mettler DSC30. For DMS, the specimens were approximately 3 × 12 × 40 mm in size and were heated from the glassy state in temperature steps of about 5°C. The strain level was 0.2–1.0% at a frequency of 1.0 Hz. Peaks in tanδ were reported as T_gs. For DSC, a 15 mg sample was heated at the rate of 10°C/min from −120 to 250°C, in an aluminum pan under a dry N_2 environment.

RESULTS AND DISCUSSION

Reaction Kinetics using FTIR

Figure 2 shows the FTIR kinetics of formation of pure PMMA and PS. Both autoacceleration and vitrification are evident from the reaction-time curves, the latter slowing the reaction at 80–90% conversion. The styrene reaction was inhibited due to traces of the residual inhibitor, 4-*tert*-butylcatechol. However, the MMA reaction curve was highly reproducible and superimposable on the corresponding curve obtained from the polymerization of vacuum distilled MMA.

Figure 3 shows the PU formation kinetics in an SIN, in bulk, and in solution with 50% toluene. The polymerization rate is highest in bulk, and lower in the remaining two cases. Possible general reasons are monomer dilution and the T-12 catalyst being

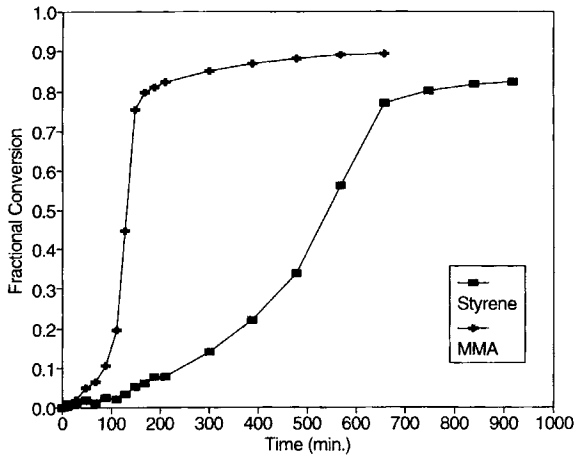

Figure 2 FTIR-kinetics of polymerization for MMA and styrene. Both with 3% crosslinker (TEGDM and DVB, respectively); and 0.5% LPO initiator. Polymerization temperature = 60°C. Note the Trommsdorff effect and subsequent vitrification in each curve.

partially soluble in the PMMA phase. In the SIN, the rate may also be lowered due to the higher viscosity of the PMMA-rich phase.

Based on the curves of Figures 2 and 3, and separately determined gelation times, the critical conversions at gelation were determined for the three homopolymers (see Table II). The PU gels at the same conversion of about 65% within experimental error regardless of dilution up to 50% in toluene. For PU, Table II also shows the theoretical critical conversion calculated using the Flory–Stockmayer statistical approach to gelation.[17] The reason for earlier experimental gelation is attributed to the formation of allophanate linkages in the PU.[18] The last column gives the molecular weight between the crosslinks, M_c, of fully cured homopolymer networks calculated from the rubbery plateau modulus from DMS, using the equation,

$$M_c = \rho RT/G^*, \qquad (1)$$

where ρ is the density, and G* represents the complex shear modulus.

Figure 4 shows the FTIR kinetics for a 50/50 PU/PMMA SIN. For this SIN, phase separation occurred after 8 min of reaction. The system gelled later, after 50 min of reaction, at a PU conversion = 55% and PMMA conversion = 2–3%. Therefore, it may be said that the gelling component at the experimental gel point is PMMA, by noting the column 4 values in Table II. The PU would be expected to gel at about 67% conversion, thus, at about 75–80 min, noting Figure 4.

In similar experiments with 50/50 PU/PS SINs, phase separation occurred first, after 80 min of reaction, followed closely by gelation of PU after 98 min of reaction. The PS gelled much later, according to the conversion–time data from FTIR.

Modulus Behavior from RDA-II and Phase Continuity

Figures 5 and 6 show, respectively, the complex shear modulus, G*, and tan δ behavior vs. temperature of two such SINs (50/50 PU/PMMA and 50/50 PU/PS) and their corresponding homopolymer networks. There are no measurable inward shifts of T_gs in either SIN. (In fact, one can see slight outward shifts in the SIN T_gs. This unexpected behavior is discussed briefly in Appendix I.) Corresponding experiments on the positions of T_gs in the various SINs were also carried out on the DSC. The results were substantially identical, in that no measurable inward shift of the T_gs was observed.

Also, both SINs were chalk white in color, the PMMA-based being slightly translucent owing primarily to the closer refractive indices of PMMA and PU, as indicated by Table III. These observations together indicate that the SINs were coarsely phase separated with almost no segmental interaction between the two polymers. Using the famous Fox equation[20] and these T_g values, less than 1% miscibility is indicated between the two polymers in each SIN from the above DMS data. This is because in both of these particular preparations, phase separation precedes gelation.

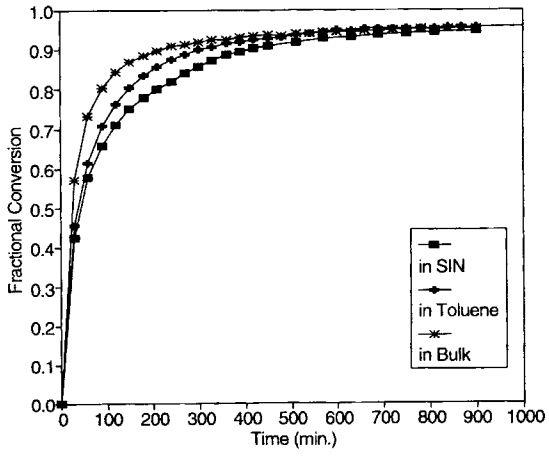

Figure 3 FTIR-kinetics of polymerization for PU in bulk, in toluene (50%) and in SIN (50% with MMA/PMMA). T-12 catalyst concentration = 0.05% (w/w PU); Polymerization temperature = 60°C.

Corresponding semi-SINs were also prepared for both systems with the PU linear. DSC results (not presented) showed two distinct T_gs, indicating coarse phase separation to almost pure polymer domains. Physically, these semi-SIN samples were sticky, cheesy, and very weak. Because stickiness, in particular, is associated with linear polymers above their T_gs, it is possible that the PU forms the continuous phase in both PS- and PMMA-based SINs at the 50/50 compositions studied.

To address the issue of continuity of the rigid networks, the 20°C modulus values of the SINs were compared with a few theoretical models that predict modulus of a polymer blend based on pure polymer moduli (see Fig. 7). Takayanagi's upper-bound model[21] applies to blends in which the rigid polymer (PS or PMMA) forms the continuous phase. On the other hand, Takayanagi's lower-bound model[21] fits blends with the softer polymer (PU) as the continuous phase. The Davies[22] and the Budiansky[23] models were developed for blends with dual phase continuity. The equations corresponding to each of these models are shown below.

Takayanagi upper-bound model:

$$G = \vartheta_1 G_1 + \vartheta_2 G_2 \quad (2)$$

Takayanagi lower-bound model:

$$G = [\vartheta_1/G_1 + \vartheta_2/G_2]^{-1} \quad (3)$$

Davies model:

$$G^{1/5} = \vartheta_1 G_1^{1/5} + \vartheta_2 G_2^{1/5} \quad (4)$$

Budiansky model:

$$\vartheta_1/[1 + \varepsilon(G_1/G - 1)] + \vartheta_2/[1 + \varepsilon(G_2/G - 1)] = 1 \quad (5)$$

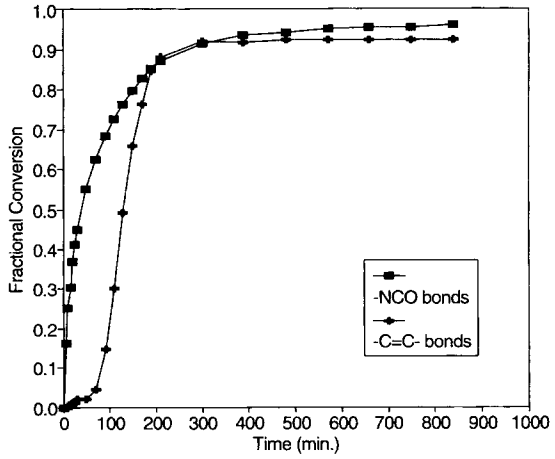

Figure 4 FTIR-kinetics of polymerization for both PU and PMMA in a 50/50 SIN. Based on PMMA, TEGDM crosslinker = 3%; LPO initiator = 0.5%. Based on PU, T-12 catalyst = 0.05%. Polymerization temperature = 60°C.

where,

$$\varepsilon = 2(4 - 5\nu_\rho)/15(1 - \nu_\rho) \quad (6)$$

and

ν_ρ = Poisson's ratio for the blend/IPN.

For all the above models,

G = shear modulus of the blend,
G_1 = shear modulus of the rigid polymer (PS or PMMA),
G_2 = shear modulus of the soft polymer (PU),
ϑ_1 = volume fraction of the rigid polymer,
ϑ_2 = volume fraction of the soft polymer.

Table II Experimental Critical Extents of Reactions at Gelation for Pure Networks (Polymerization Temp. = 60°C).

Sample	Description	Gelation Time (min)	Conversion at Gelation (p_c) (%)	Fully Polymerized M_c[a] (g/mol)
PMMA-1	3% TEGDM	25	2	3600
PMMA-2	0.5% TEGDM	68	8	5200
PS	3% DVB	110	2	3000
PUR-1	0.05% T-12	40	67	2600
PUR-2	0.05% T-12 (w/50% toluene)	68	64	—
PUR-3	statistical theory	—	82	—

[a] Calculated from the rubbery plateau modulus, G*, from RDA-II data.

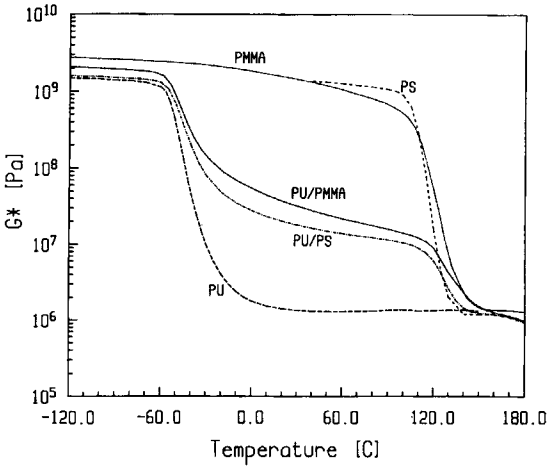

Figure 5 Dynamic shear modulus vs. temperature behavior for 50/50 SINs of PU/PMMA and PU/PS, along with the corresponding homonetworks. SINs show coarse phase separation without any inward shifts of T_gs. Frequency = 1 Hz.

According to Figure 7, the moduli for both PU/PMMA and PU/PS 50/50 SINs lie between those predicted by the models for a continuous PU phase [Takayanagi's lower-bound, curve (d)] and dual phase continuity [Davies and Budiansky, curves (b) and (c), respectively]. This may indicate a morphology with a continuous PU phase with lesser degrees of continuity for the rigid networks in each of the two SINs analyzed here. Although the moduli for pure PS and PMMA are substantially the same (1.44×10^9 Pa, at 20°C), their 50/50 SINs with

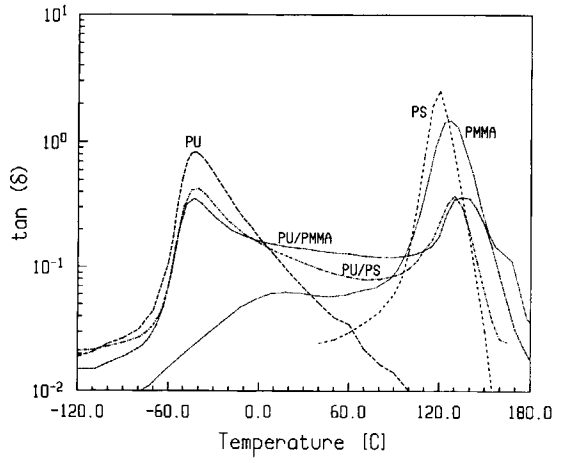

Figure 6 Logarithmic loss tangent vs. temperature for 50/50 SINs of PU/PMMA and PU/PS, along with the corresponding homonetworks. SINs show coarse phase separation without any inward shifts of T_gs. On the contrary, very slight outward shifts may be seen for some SIN peaks. Frequency = 1 Hz.

Table III Refractive Index Values for the Three Polymers Under Study.

Polymer	Refractive Index (20°C)
PU[a]	1.46
PMMA[b]	1.49
PS[b]	1.59

[a] PU value was calculated as the weighted average of the refractive indices (20°C) of the two major components, polyoxypropylene and H_{12}MDI, which have R.I. values of 1.4495 (ref. 19) and 1.4977 (data from supplier), respectively. The two components, respectively, constitute 76.5% and 20.0% of the PU by weight. The remainder 3.5% is TMP, which is neglected in the present calculation.

[b] PMMA and PS values were taken from ref. 19.

PU are not, the PU/PMMA SIN being slightly higher. This may be explained in terms of the difference in the order of critical events during their polymerizations. For PU/PMMA SINs, the order was:

$$\text{Phase Separation} \rightarrow \text{Gelation of Rigid polymer (PMMA)} \rightarrow \text{Gelation of Elastomer (PU)} \quad (7)$$

whereas, for PU/PS SINs, the order was:

$$\text{Phase Separation} \rightarrow \text{Gelation of Elastomer (PU)} \rightarrow \text{Gelation of Rigid polymer (PS)} \quad (8)$$

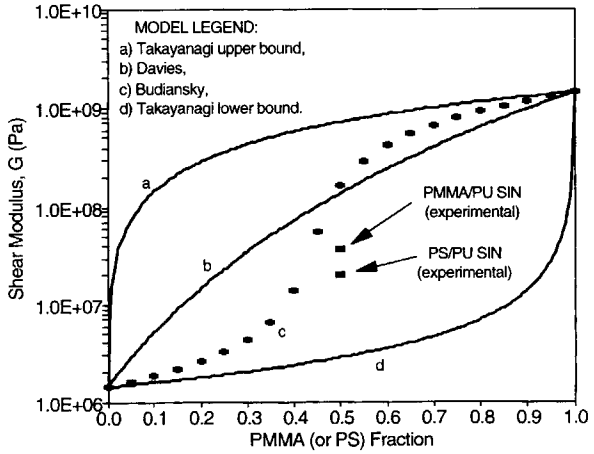

Figure 7 Shear moduli at 20°C of 50/50 SINs of PU/PMMA and PU/PS shown (■) along with four theoretical models. Model (a) represents a continuous rigid phase; models (b) and (c) represent dual phase continuity; and model (d) represents a continuous softer phase.

Preliminary Phase Diagrams

Figure 8 shows the phase diagram for the MMA–PMMA–"U" ternary system determined from premixed materials with the low MW linear PMMA (IRD-2) at 20°C and at 60°C. The system becomes more miscible at higher temperatures, suggesting an upper critical solution temperature (UCST) behavior. It may also be noted that the immiscible compositions at 20 and 60°C were miscible and single phased at 100°C, further evidence of a UCST behavior.

Metastable Phase Diagrams

MMA–PMMA–"U"

Figure 9 shows the phase diagram at 60°C determined by *in situ* polymerization of MMA in presence of "U," for linear [curve (3)], as well as for crosslinked PMMA (w/0.5% TEGDM) [curve (4)]. For comparison, curve (2) of Figure 8 for the low MW linear PMMA (M_n = 42,000 g/mol; GPC) is also shown. Comparing the two curves for linear PMMA [curves (2) and (3)] shows that increasing the PMMA molecular weight decreases the miscibility by shifting the envelope to the left (M_n for *in situ* polymerized PMMA = 385,000 g/mol, by GPC). Also, comparing the two *in situ* curves [(3) and (4)] shows that crosslinking the PMMA decreases miscibility further, shifting the envelope even more to the left. In another IPN system, poly(vinyl methyl) ether/polystyrene sequential IPNs, Bauer et al.[24,25] as well as Fay et al.[26] have also found that presence of crosslinks tends to decrease miscibility as compared to the corresponding linear blends.

For the *in situ* experiments, the extent of undesirable polymerization of "U" to PU was also determined from the FTIR data. The PU conversion at phase separation was typically 10–15% or less, which was assumed to have a negligible effect on the phase diagram curves such as (3) and (4) of Figure 9.

The phase diagram with crosslinked PMMA [curve (4) of Fig. 9] is better referred to as a metastable phase diagram, because the SIN system is not expected to achieve complete thermodynamic equilibrium due to the crosslinked structure. Instead of reaching a true thermodynamic equilibrium, such a system may be said to reach a metastable equilibrium. A possible state of affairs is the condition at which the thermodynamic forces of phase separation are exactly counterbalanced by the mechanical constraints of the network structure. These "mechanical constraints" may be related to the forces of rubber elasticity because when a polymer segment is pulled towards a growing domain, its complete network

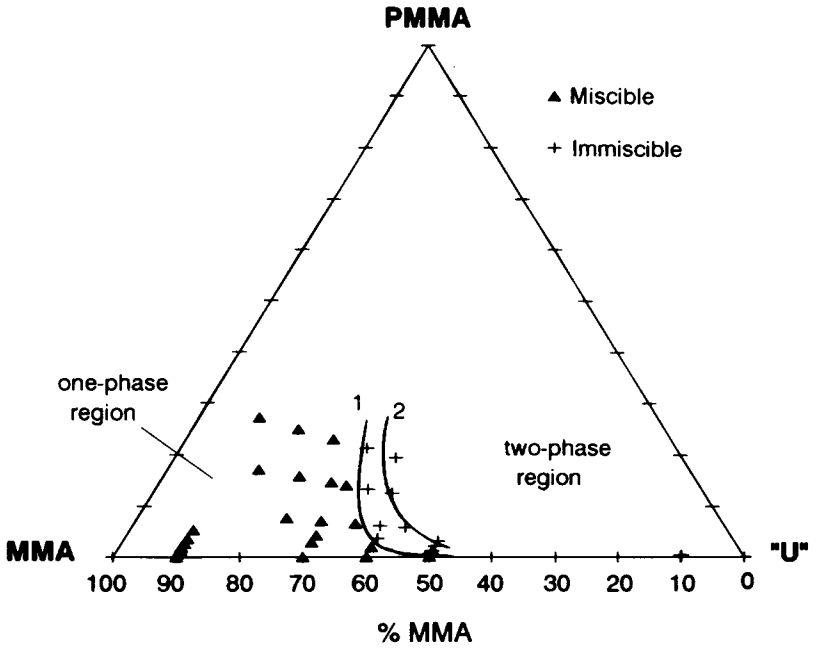

Figure 8 Ternary phase diagrams for the system MMA–PMMA–"U" determined by the premixed method, using linear PMMA (M_n = 42,000 g/mol). No polymers/prepolymers are crosslinked in this diagram. (1) at 20°C; (2) at 60°C. Experimental points are shown only for curve (1) to avoid complexity of the Figure.

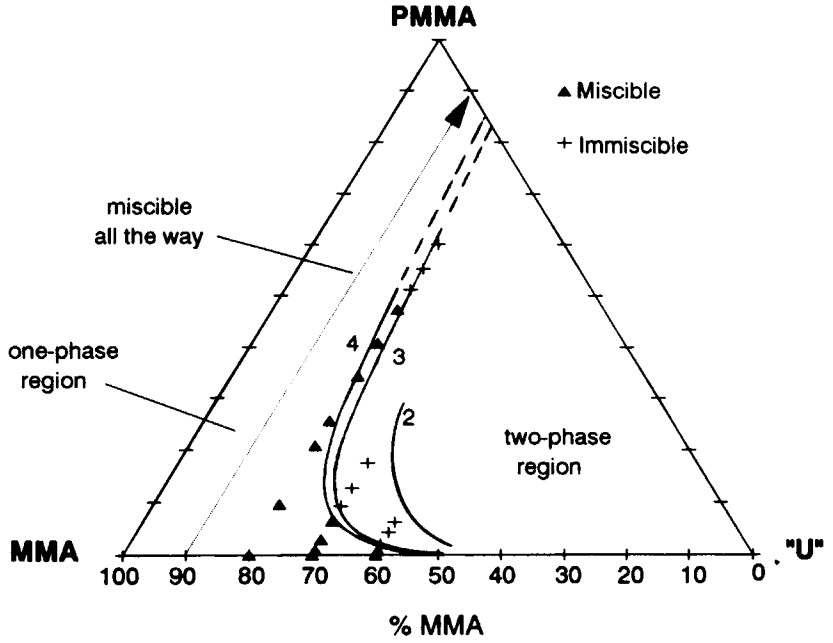

Figure 9 Metastable ternary phase diagrams at 60°C for the system MMA–PMMA–"U" determined by polymerizing the PMMA *in situ*: (3) linear PMMA, M_n = 385,000 g/mol; (4) crosslinked PMMA, M_c = 5200 g/mol. For comparison, the 60°C curve (2) from Figure 8 (M_n = 42,000 g/mol) is also shown. Experimental points are shown only for curve (3) to avoid complexity.

may act against it. Therefore, in concept, the magnitude of these mechanical constraints could be estimated using the rubber elasticity theory. Furthermore, the kinetics of phase separation are slow because of the high viscosity and/or vitrification, also resulting in a lag with respect to the thermodynamic equilibrium, as found by Zhou et al.[14] This deviation from equilibrium may also be taken into account while defining a metastable phase equilibrium. In either case, however, the curves, while probably displaced slightly, serve to describe the general features of the system.

The development of curve (4) in Figure 9 is shown in more detail in Figure 10. The gelation of PMMA can be represented by a line G_1–"U" corresponding to 8% conversion of MMA to PMMA (see Table II) (the possible deviation of this gelation line from the straight line G_1–"U" is briefly discussed below near the end of this section). The MMA–PMMA mix is a sol below this line and a gel above it. It can be seen that the phase separation curve and this gelation line have an intersection which is a critical point, "A," representing simultaneous phase separation and PMMA gelation.

Experimental reaction paths are shown for this diagram as lines with arrows. For the reaction starting with 60% MMA, phase separation occurs before gelation, whereas on starting with 80% MMA, it occurs after gelation. For 70% MMA at the start, both events occur nearly simultaneously. The difference is indicated by the near chalk-white appearance of the material resulting from the right of the critical point "A," as compared to the translucence of material polymerized to the left of the critical point, suggesting that gelation before phase separation restricts domain size.

An interesting modification of the synthesis scheme would be when the MMA polymerization is initiated photochemically at room temperature, instead of thermal initiation at higher temperatures. In that case, the polymerization of "U" to PU may be restricted even in the presence of the T-12 catalyst by keeping the temperature low until the PMMA network is completely formed. (Such a polymerization scheme has been appropriately named an "*in situ* sequential" IPN synthesis, by Meyer and co-workers.[27]) Subsequent heating will activate the polymerization of "U." If the initial MMA/"U" ratio is greater than 70/30, then according to Figure 10, the polymerization path would lie to the left of the critical point "A," and order of the events would become:

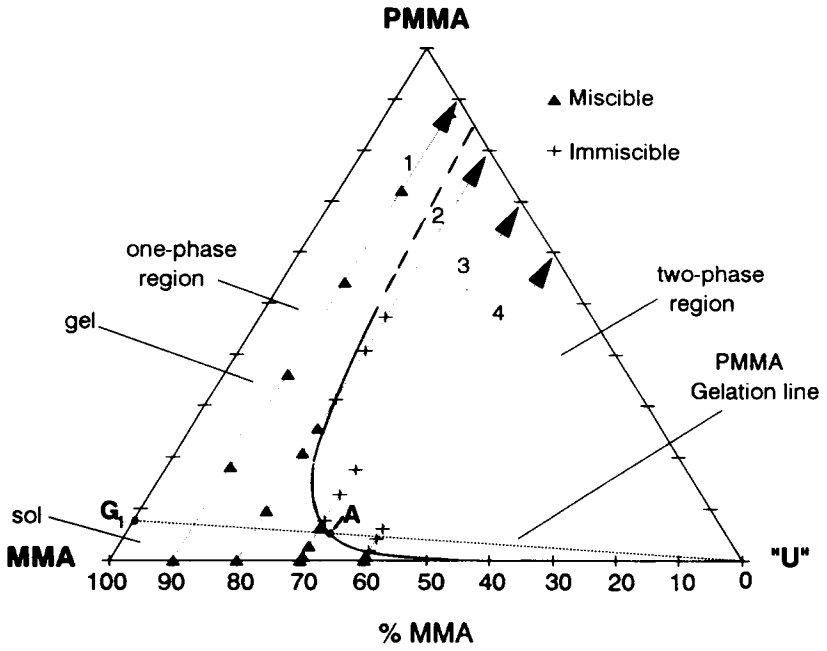

Figure 10 Metastable ternary phase diagram for the system MMA–PMMA–"U" determined by polymerizing the cross-PMMA *in situ* [same as curve (4) of Fig. 9]. The line of gelation for PMMA is shown as "U"-G_1 along with the critical point, "A." Four reaction paths are shown: (1) gels and never phase separates; (2) gels first, phase separates later; (3) simultaneous phase separation and gelation of PMMA; and (4) phase separates first, gels later.

Gelation of Rigid polymer (PMMA) → Phase Separation → Gelation of Elastomer (PU) (9)

This possibly results in a continuous cross-PMMA matrix with a dispersed cross-PU phase, which might behave like a rubber-toughened cross-linked PMMA. However, if the initial MMA/"U" ratio is less than 70/30, then the polymerization path would lie to the right of the critical point "A," and will follow the order shown above for the 50/50 SIN of PU/PMMA [eq. (7)].

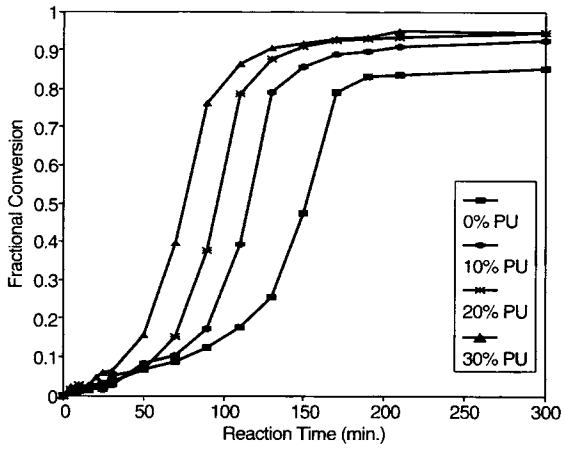

Figure 11 FTIR polymerization kinetics for the formation of cross-PMMA in the presence of linear PU in various proportions. Note faster polymerizations with increasing "dilution" by PU. Temperature = 60°C; TEGDM = 0.5% based on PMMA; LPO = 0.5% based on PMMA.

MMA–PMMA–PU

The corresponding metastable phase diagram for the MMA–PMMA–PU system was developed by employing the *in situ* technique using a linear PU prepared with BEPD chain extender as described in the experimental section. The polymerization kinetics for MMA in the presence of linear PU at different concentrations are shown in Figure 11. It would be expected that the polymerization would get slower as the MMA reaction mixture is "diluted" by the presence of PU. However, the exact opposite is noticed in the PU concentration range studied here. Meyer et al.[27] have explained similar behavior observed in their *in situ* sequential PU–PMMA IPNs by proposing that the higher viscosity due to the presence of PU during formation of PMMA decreases the chain termination rate in comparison to the chain propagation rate, resulting in an earlier onset of the autoacceleration effect.[17]

The metastable phase diagram for the ternary system MMA–PMMA–PU is shown in Figure 12. The data resulted in an unexpected rise in the phase separation curve, as seen near 70% MMA on the base of the triangle. This may also be an artifact arising due to the variable viscosity of the reaction mixtures, because ordinary thermodynamics would not predict such a rise. The extrapolation of the phase separation curve (dashed lines) is done hypothetically up to the line PU–PMMA, keeping the overall shape of the curve same as that for the curve of Figure 10. The curve is made to meet the line PU–PMMA at points representing less than 1% miscibility between the two polymers (which was indicated by the glass transition data above). Note that the lines PU–MMA and PMMA–MMA are expected to lie completely in the one-phase region of the diagram.

In all the experiments shown in Figures 11 and 12, phase separation occurred before gelation of PMMA. In fact, the reaction mixture did not totally lose its fluidity at the expected gelation time (corresponding to 8% PMMA conversion). Instead, it acquired the consistency of "broken yogurt" or a gel that is broken on the scale of the mold (vial). This might mean that on gelation, the PMMA formed the less continuous phase, as noted previously in Figure 7. Note that similar to the diagram of Figure 10, there must be a critical point, "B" for this diagram too, representing simultaneous phase separation and PMMA gelation.

Metastable Four-Component Phase Diagram: MMA–"U"–PMMA–PU

Figure 13 shows the metastable phase diagram of all four SIN components (two monomers and two polymer networks, MMA–"U"–PMMA–PU) as a tetrahedron in three dimensions (3D). Each of the four triangular faces of this tetrahedron represents a metastable ternary phase diagram (in 2D), two such already shown in Figures 10 and 12. The phase separation curves in the 2D triangular diagrams of Figures 10 and 12 can be logically seen as sections of the phase separation surface in the 3D diagram, see curves C–D–A–E in the front left triangle, and curve J–B–K–L in the rear triangle. The phase separation surface, then, is defined by the points C–D–A–E–L–K–B–J. Similarly, the PMMA gelation lines of the ternary diagrams are actually sections of the PMMA gelation plane, G_1–"U"–PU, in the tetrahedron.

It may be noted that the diagram is shown here with the curves and surfaces slightly moved from their end points, J, L, E, etc., to ease visualization, maintaining, however, its overall qualitative fea-

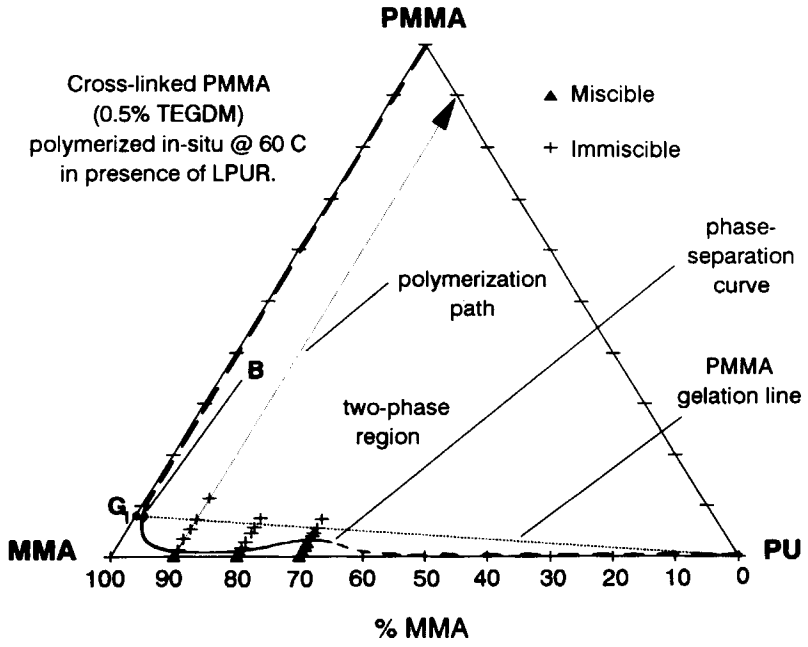

Figure 12 Metastable ternary phase diagram for the system MMA–PMMA–PU determined by polymerizing cross-PMMA *in situ* with linear PU. Temperature = 60°C. The line of gelation G_1–PU is primarily based on the gelation line of Figure 10. A typical MMA polymerization path is also shown using an arrow.

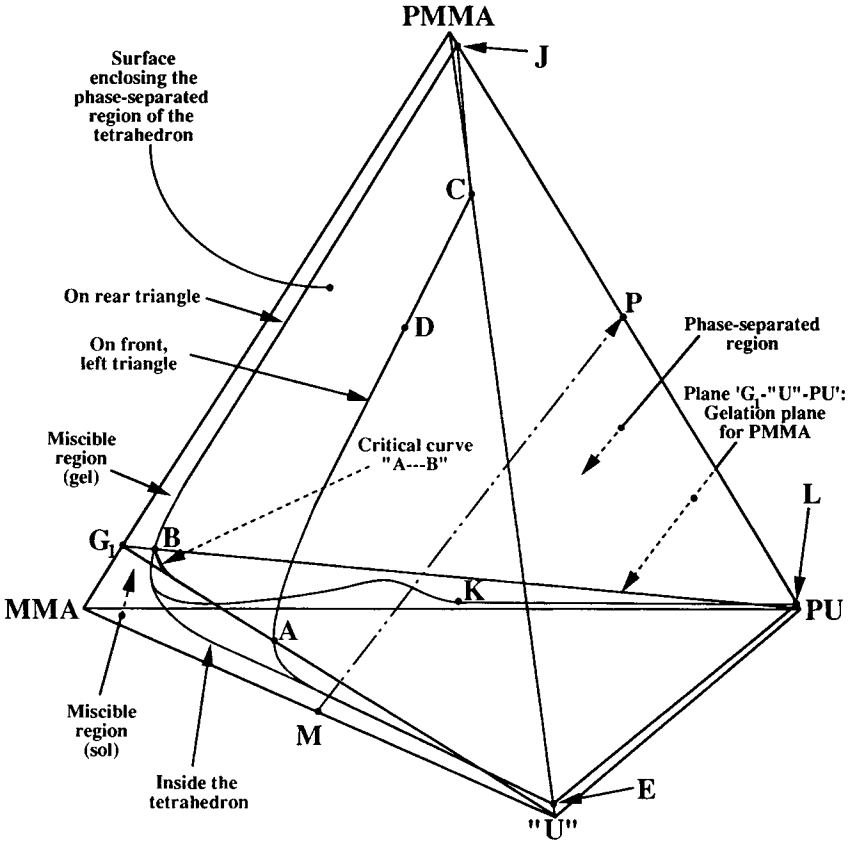

Figure 13 Metastable phase diagram for the SIN representing both polymers, PU and PMMA, and corresponding monomer mixtures, MMA and "U." Temperature = 60°C. The PMMA gels on and above the plane G_1–"U"–PU. The surface enclosing the phase-separated region in the tetrahedron is marked. Especially note the intersection of the PMMA gelation plane and this surface along the curve A–B, representing the condition of simultaneous phase separation and PMMA gelation.

tures. The intersection of the phase separation surface with this plane forms a critical curve shown "A–B" in Figure 13. The significance of this critical curve is the same as that of the critical points A and B of Figures 10 and 12, as described above. A reaction path to its left sees PMMA gelation first, followed by phase separation, whereas one to its right sees the reverse.

The bottom face, MMA–"U"–PU is seen to be entirely one phased for this system, noting the prolific use of its miscibility in the synthesis of PU–PMMA IPNs, both sequentially and simultaneously.[2–13] The remaining, right face, PMMA–PU–"U," is almost entirely phase separated except between lines E–L and "U"–PU, and in the small region enclosed by points PMMA–J–C.

Figure 14 shows the gelation plane of PU bounded by points G_2–MMA–PMMA, where the point G_2 represents 67% PU conversion in bulk. The intersection of the two gelation planes forms a critical line G_1–G_2, representing the simultaneous gelation of PMMA and PU for the crosslinker levels used. Simultaneous gelation in SINs is a particularly interesting condition, which was thought to promote dual-phase continuity (see the work of Touhsaent et al.[28,29]). In the present system, however, this condition can be achieved only after phase separation, because the line G_1–G_2, lies for the most part, in the two-phase region (volume) of the tetrahedron. Note that very close to the point G_1, where the line G_1–G_2 does lie in the one-phase region, the PU may actually never gel because it is extremely diluted by the MMA mix, the line G_1–G_2, therefore, dotted. Similarly, the PMMA may never gel because of its extreme dilution by the "U" mix in the other extreme of the tetrahedron, near the line "U"–PU. In fact, a better representation of the gelation planes may be with a slight deviation from the ideal planar structure, shown here for simplicity. For example, the PMMA plane may bend slightly upwards near

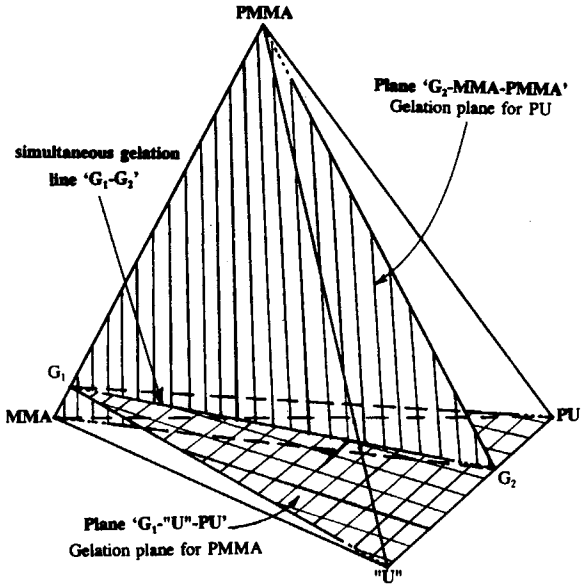

Figure 14 The four component composition diagram for the same PU/PMMA SIN system as in Figure 13, showing the two gelation planes. Plane G_1–"U"–PU represents gelation of PMMA at 8% conversion, and plane G_2–MMA–PMMA that of PU at 67% conversion.

the points "U" and PU, so that it actually meets the lines PMMA–"U" and PMMA–PU at points slightly above points "U" and PU, respectively.

DISCUSSION

Substantially the same PU/PMMA system yielded different morphologies in different studies described in the literature.[3-13] In this study, it is shown that these differences can arise from differences in the polymerization routes, which contain three important events: gelation I, gelation II, and phase separation of polymer I from polymer II.

Defining a metastable phase equilibrium for SINs and IPNs allows the development of a 3D metastable phase diagram as a tetrahedron. This subsequently allows visualization of the course of events during SIN formation and provides direction for controlling the specific order of events. For many SIN applications, it is desired that phase separation occurs after at least one component gels. Starting from point "M," representing the initial monomer mixture, on the line MMA–"U" in Figure 13, one may choose different paths leading to the three important events mentioned above.

For example, PU-gelation can be achieved first by moving along the bottom face of the tetrahedron, MMA–"U"–PU, by polymerizing the PU alone, until the PU–gelation plane is crossed, via a type of *in situ* sequential IPN synthesis. Similarly, PMMA–gelation may be achieved first, provided monomer composition relative to the position of critical point "A" is suitable, by moving along the front left face, MMA–"U"–PMMA. This may be done as described above, by polymerizing MMA using photoinitiation at a low temperature, so that the PU formation rate can be kept low enough, until the PMMA–gelation plane is crossed. Finally, it is easiest to achieve the phase separation first. All that is needed is to simultaneously form both PU and PMMA at comparable rates, perhaps following the line M–P in Figure 13.

Although not shown in Figures 13 and 14, a triple critical point exists where the line G_1–G_2 of Figure 14 intersects the critical curve "A–B" of Figure 13. This point represents the simultaneous occurrence of all three events, phase separation, and both polymers' gelations.

Although the data presented herein are for the PU–PMMA system at specific crosslinker levels, the concepts underlying Figures 13 and 14 are perfectly general and should work for other systems as well. Somewhere in the faces and in the interior regions of the corresponding figures will lie the gelation planes of the two polymers, and the surface of phase separation. The planes need not be flat, but may be curved, as is the surface C–D–A–E–L–K–B–J in Figure 13. The relative positions of these curves and planes, and their intersections are controlled by the thermodynamics of mixing, the interfacial surface tension, and the crosslinker level of both polymer networks.

CONCLUSIONS

The process of SIN synthesis has been described as being composed of three important events: gelation of polymer I, gelation of polymer II, and phase separation of polymer I from polymer II. It is important to identify the order in which these three events occur in any SIN system and, if possible, control their order of occurrence to manage the resulting morphology and properties.

Metastable phase diagrams were first constructed for the ternary systems MMA–PMMA–"U" and MMA–PMMA–PU. Also shown are the gelation lines for PMMA in these triangles. The intersection of the gelation line with the phase separation curve has been identified as a critical point that plays an important role in the development of morphology.

Similarly, the complete SIN system, MMA–"U"–PMMA–PU, composed of the two monomers and the corresponding two polymer networks, has been represented in the form of a tetrahedron in three dimensions. A phase separation surface divides the tetrahedron into a miscible region (volume) and an immiscible region (volume). The gelations of the two polymers can be represented by two planes that intersect, forming a line representing the condition of simultaneous gelation. Finally, one gelation plane (PMMA) also intersects with the phase separation surface to form a critical curve "A–B," important in terms of the development of morphology and properties of the SIN.

APPENDIX I

Abnormal Outward Shifts in SIN T_gs

There are several possible causes for the abnormal outward shifts in the T_gs of the SINs noted in Figures 5 and 6 and it is possible that more than one of the following explanations are valid.

One possible explanation involves thermal and pressure effects. When the samples are quenched from the high curing temperatures down to lower room temperatures, both phases contract, but to different extents. The soft PU (above T_g) will have a higher thermal coefficient of expansion than the rigid PMMA or PS (below T_g), and will tend to shrink more than the PMMA (or PS). Due to the pressure imbalance thus created across the two phases, the PU phase would become slightly stretched and the PMMA phase slightly compressed. Thus, according to the free volume theory, the PU T_g is lowered, while the PMMA T_g is raised.

Another possible reason (only for the lowering of the PU T_g) is that the PU conversion may be limited even after postcuring due to the presence of the rigid PMMA. This will reduce the PU T_g from its fully cured value.

A third possible explanation (only for the rise in PMMA T_g) is based on the zone-refining theory[30] according to which, some low MW species of the rigid polymer may preferentially dissolve in the soft PU phase. This will tend to increase the T_g of the remaining rigid phase.

Financial support from 3M Company for this work in the form of a Fellowship for V.M. is greatly appreciated. The authors are also thankful to Dr. S. Siranovich of Miles Inc. for providing samples of Desmodur W (diisocyanate), along with some helpful suggestions toward its use, and to Eastman Chemical Co. for providing BEPD (diol) samples. The authors also acknowledge the assistance of Mr. W. R. Anderson in setting up the FTIR experiments. F.D.P. acknowledges the NFWO for financial support.

REFERENCES

1. D. Klempner, L. H. Sperling, and L. A. Utracki, Eds., *Interpenetrating Polymer Networks,* ACS Books, Advances in Chemistry Series 239, American Chemical Society, Washington, DC, 1994.
2. L. H. Sperling and V. Mishra, in *The 25th Anniversary Symposium of the Polymer Institute,* University of Detroit-Mercy, September '94, Technomic Press, Lancaster, PA, 1994.
3. S. C. Kim, D. Klempner, K. C. Frisch, W. Radigan, H. L. Frisch, *Macromolecules,* **9**(2), 258 (1976).
4. S. C. Kim, D. Klempner, K. C. Frisch, H. L. Frisch, *Macromolecules,* **9**(2), 263 (1976).
5. I. Hermant and G. C. Meyer, *Polymer,* **24,** 1419 (1983).
6. A. Morin, H. Djomo, and G. C. Meyer, *Polym. Eng. Sci.,* **23**(7), 394 (1983).
7. T. Hur, J. A. Manson, R. W. Hertzberg, and L. H. Sperling, *J. Appl. Polym. Sci.,* **39,** 1933 (1990).
8. T. Hur, J. A. Manson, R. W. Hertzberg, and L. H. Sperling, in *Multiphase Polymers: Blends and Ionomers,* L. A. Utracki and R. A. Weiss, Eds., ACS Symposium Series, Washington, DC, 1989, p. 395.
9. M. Akay and S. N. Rollins, *Polymer,* **34**(5) 967, (1993).
10. M. Akay and S. N. Rollins, *Polymer,* **34**(9), 1865 (1993).
11. H. L. Frisch, P. Zhou, K. C. Frisch, X. H. Xiao, M. W. Huang, and H. Ghiradella, *J. Polym. Sci., Part A: Polym Chem.,* **29,** 1031–1038 (1991).
12. M. T. Tabka, J. M. Widmaier, and G. C. Meyer, *Plastics, Rubber and Composites Processing and Applications,* **16,** 11–16 (1991).
13. M. T. Tabka, J. M. Widmaier, and G. C. Meyer, in *Sound and Vibration Damping with Polymers,* R. D. Corsaro and L. H. Sperling, Eds., ACS Symposium Series No. 424, American Chemical Society, Washington, DC, 1990.
14. P. Zhou and H. L. Frisch, *J. Polym. Sci., Part A: Polym. Chem.,* **31,** 3479 (1993).
15. H. L. Frisch and P. Zhou, *J. Polym. Sci., Part A: Polym. Chem.,* **31,** 1967 (1993).
16. H. L. Frisch, *New. J. Chem.,* **17,** 697 (1993).
17. G. Odian, *Principles of Polymerization,* 3rd Ed., Wiley, NY, 1992.
18. C. Hepburn, *Polyurethane Elastomers,* Applied Science, UK, 1982, p. 4.
19. L. Bohn, in *Polymer Handbook,* 2nd Ed., J. Brandrup and E. H. Immergut, Eds., Wiley, New York, 1974, pp. III-241.
20. T. G. Fox, *Bull. Am. Phys. Soc.,* **1,** 123 (1956).

21. M. Takayanagi, *Mem. Fac. Eng. Kyushu Univ.*, **23,** 11 (1963).
22. W. E. A. Davies, *J. Phys. D* **4,** 318 (1971).
23. B. Budiansky, *J. Mech. Phys. Solids,* **13,** 223 (1965).
24. B. J. Bauer, R. M. Briber, and C. C. Han, *Macromolecules,* **22,** 940 (1989).
25. B. J. Bauer and R. M. Briber, in *Advances in Interpenetrating Polymer Networks,* Vol IV, D. Klempner and K. C. Frisch, Eds., Technomic, Lancaster, PA, 1994.
26. J. J. Fay, C. J. Murphy, D. A. Thomas, and L. H. Sperling, in *Sound and Vibration Damping with Polymers,* R. D. Corsaro and L. H. Sperling, Eds., ACS Symposium Series, No. 424, American Chemical Society, Washington, DC, 1990.
27. S. R. Jin, J. M. Widmaier, and G. C. Meyer, *Polymer,* **29,** 346 (1988).
28. R. E. Touhsaent, D. A. Thomas, and L. H. Sperling, *J. Polym. Sci., Polym. Symp.,* **46,** 175–190 (1974).
29. R. E. Touhsaent, D. A. Thomas, and L. H. Sperling in *Toughness and Brittleness of Polymers,* R. D. Deanin and A. M. Crugnola, Eds., Advances in Chemistry Series, No. 154, American Chemical Society, Washington, DC, 1976.
30. L. M. Robeson, Air Products and Chemicals, private communication.

Received September 7, 1994
Accepted October 1, 1994